Arabian Journal of Chemistry (2016) 9, S1755–S1764

King Saud University

Arabian Journal of Chemistry

www.ksu.edu.sa
www.sciencedirect.com

ORIGINAL ARTICLE

Nanophotocatalytic UV degradation system for organophosphorus pesticides in water samples and analysis by Kubista model

Amit Kumar Sharma *, Rajeev Kumar Tiwari, Mulayam Singh Gaur

Department of Physics, Pesticides Research and Sensors Laboratory, Hindustan College of Science and Technology, Farah, Mathura 281 122, U.P., India

Received 5 December 2011; accepted 27 April 2012
Available online 7 May 2012

KEYWORDS

Nanophotocatalyst;
OP pesticides;
Photolysis;
Electrical energy efficiency;
Quantum yield

Abstract The photocatalytic degradation of organophosphorus pesticides like methyl parathion (MP) and parathion (PA), under UV irradiation is studied using synthesized Zinc oxide (ZnO) nanocatalyst. Two cases were considered for removal of organophosphorus (OP) pesticides such as only UV (i.e. direct photolysis) and UV–ZnO nanocrystal. The Langmuir–Hinshelwood (L–H) relationship between the initial rate and the initial concentration indicates that the reaction occurs with the adsorbed substrate. Factors affecting the kinetics of the process such as quantum yield, electrical energy per order (E_{EO}), dosage of nanophotocatalyst and L–H model have been discussed. The optimal conditions for degradation were obtained using 85 mg l^{-1} ZnO, 40% O_2 (v/v) with rate constants L–H adsorption equilibrium constant (K_p = 0.127 for MP and 0.122 for PA) and rate constant of surface reaction (K_c = 0.212 for MP and 0.204 for PA). The kinetics of disappearance of OP pesticides (i.e. MP and PA) in water suspension using ZnO nanophotocatalyst illuminated at λ = 253.7 nm and examined. The quantum yield values for photodegradation of pesticides by photolysis and UV–ZnO process under the illumination of UV at 253.7 nm is calculated as 0.00072, 0.012 for MP; 0.00068 and 0.01 for PA. The E_{EO} values for degradation of pesticide by photolysis for UV–ZnO was found to be 20,006, 1392.4 kWh m^{-3} for MP; 19,089 and 1387.2 kWh m^{-3} for PA.

1. Introduction

The photochemical reaction comprises a series of events starting from the initial act of light absorption and ending in the production of stable molecules generally different from the reactant molecules. Recently, a computational model has been reported on OP pesticide effects with different metabolic proteins in human by Sharma et al. (2011). In general, light sources, windows and actinometers for vacuum ultraviolet photochemical studies of toxic pesticides are described (Ollis

* Corresponding author. Fax: +91 0565 2763364.
E-mail addresses: amit_vashishtha1980@rediffmail.com, amit.db1980@gmail.com (A.K. Sharma).
Peer review under responsibility of King Saud University.

Production and hosting by Elsevier

http://dx.doi.org/10.1016/j.arabjc.2012.04.044
1878-5352

and Al-Ekabi, 1993; Stephen et al., 2000). The photocatalytic transformation of the insecticide chlorpyrifos *O*,*O*-diethyl-*O*-(3,5,6-trichloro-2-pyridinyl) phosphorothioate has been studied by Sulaiman Gafar Muhamad (2010). Time dependent studies of atom or molecule or compound with concentrations follow the decay of absorption intensity or resonance intensity. Trace amount of pesticide may threaten human health remaining in the environment. Different pathways of organophosphorus decomposition such as hydrolysis (Doong and Chang, 1997), photolytic oxidation (Dannenberg and Pehkonen, 1998) microbial transformations (Feed et al., 1979) biological processes (Racke et al., 1992) have been reported. The degradation of phosphorothioate and phosphorodithioate subgroups of the OP pesticides, the thiophosphate functionality (P = S) can be oxidized to its corresponding oxon (P = O) (Pehkonen and Zhang, 2002). Efficient photodegradation of different pesticides was obtained using high energy lasers working at different wavelengths (Cassano et al., 1995; Chandrasekhar, 1960; Zhang and Pehkonen, 1999; Canle et al., 2001; Salari et al., 2005; Trebse and Franko, 2002). An alternative for the treatment of the waste water is electron beam irradiation in combination with other conventional treatment stages (Nicole et al., 1990; Pareek et al., 2001). This combination has been reported to remove organic dyes, heavy metals, phenols, environmental pollutants, etc. (Han et al., 2002). In the electron beam process the organic materials react with the radicals generated by water radiolysis and the degradation products can be easily removed by conventional biological or chemical treatment (Pikaev et al., 1997). The application of exciter lasers as a light source of light different chemical transformations, such as photo-polymerization and crosslinking was reported particularly, because they produce monochromatic radiation of high intensity. While nitrogen laser, providing an emission line at 227 nm, the most frequent lasers in chemistry are the exciter laser (XeCl laser at 308 nm) and the Nd: YAG laser (1060, 530, 355 nm) (Eleni et al., 2007). In another way, spectroscopic methods are in general simple, highly sensitive and very appropriate for the study of chemical reactions in the solution. However, in different cases, the peak band responses in the spectra have two or more components overlap and the analysis is no longer forward. A common approach has been single-point measurements at a wavelength where one compound dominates the spectral response and the contributions from the other compound are neglected by the use of chemometrics methods (Fouassier, 1989).

Spectral curve deconvolution or multivariate curve resolution methods are chemometrics, which concern with the pure spectra of compounds involved in the reaction and its corresponding concentration of compounds are classified into two ways: modeling methods and self-modeling methods. Kankare is the originator of the modeling method (Lopez et al., 2000, 2003; Primo et al., 2007), while other researchers have been tried to develop this method (Gooijer and Mank, 1989; Lavine, 2000; Kankare, 1970). Self-modeling methods extract the concentration profiles without having any information about the shape of the spectra. Several self-modeling approaches have been developed by Lawton and Sylvestre (1971), among these some are factor analysis based methods such as automated spectral isolation (ASI), alternative least squares (Frans and Harris, 1985), iterative target transformation factor analysis (ITTFA) (Shrager, 1986). The degradation of organophosphorous pesticides using TiO_2 and ZnO photocatalysis have been previously investigated (Lin and Liu, 1978; Diaz-Cruz et al., 1999). However, no significant effort has been made in evaluating the photocatalytic efficiency of nanophotocatalyst on organophosphorus pesticides degradation and the factors affecting it with suitable combination of Kubista model.

Therefore, we are first time reporting about the ability of spectroscopic technique with Kubista model using ZnO nanophotocatalyst and further the spectroscopic results are validated by chromatographic techniques (i.e. HPLC). The other studies were also performed like synthesis of ZnO nanocatalyst, pH effect in water matrix, L–H analysis, evaluate electrical energy per order and quantum yield for direct photolysis (UV degradation) and also with nanophotocatalyst (UV–ZnO); investigation of the efficiency of photocatalytic process in the water sample containing pesticides, and analysis by UV–Vis spectroscopy coupled with Kubista model. Further, the obtained results were validated by high performance liquid chromatography. All these factors are necessary to provide an overall evaluation of the efficiency of the UV degradation using ZnO nanophotocatalyst.

2. Experimental

2.1. Apparatus and reagents

Methyl parathion and Parathion (99.9%, purchased from Sigma–Aldrich, Germany) were prepared in methanol. The other regents such as methanol, zinc sulfate and sodium hydroxide are supplied by Merck, India. UV–Vis spectra of all samples were recorded by Hitachi U-2800 double beam spectrophotometer equipped with 10 mm quartz cells. The UV-solution 2.1 software was used to collect the absorbance data of the solution into a spreadsheet. A Shimadzu HPLC with diode $x \times y$ array solvent delivery system controller (LC-10; C_{18} column) was used for all photodegradation residue analysis.

2.2. Kubista model

In the spectral data, a series of observations were taken with time domain UV-light source (30 W lamp) with the time interval of 10 min. The collected data were presented in a data matrix (M) with dimension, x being the number of data points per spectrum and y being the number of spectra collected at various reaction time intervals. The recorded absorbance at a wavelength is assumed to be the sum of contributions of all coefficients:

$$m_j(\lambda) = \sum_{i=1}^{k} S_i(\lambda) C_{ij} (j = 1, n) \quad (1)$$

where k is the absorbing components in the reaction system, $m_j(\lambda)$ is the spectrum of organophosphorus pesticide sample j, C_{ij} is the concentration of coefficient i in sample j and n is the number of irradiated samples of organophosphorus compound. Since the Eq. (1) can be written in a matrix form as $M = x \times y$, where A is a $x \times$ k matrix of the molar absorbance and B is a $k \times y$ matrix containing concentration of samples. To carry out the curve resolution procedure on the data matrix M, the number of coefficients (k) present in the system is estimated by factor analysis (Gemperline, 1986 and Malinowski,

1991). The data matrix was decomposed to row and column matrices by singular value decomposition (SVD).

$$M = RC \tag{2}$$

where R contains the orthonormal eigen vectors spanning the row space of original data matrix and C spans the column space. A 2×2 transformation matrix (T) and its transpose (T^{-1}) are introduced to transform the matrices R and C into the real matrices x and y:

$$M = (RT)(T^{-1}C) = x \times y \tag{3}$$

$$T = \begin{bmatrix} t_1 & t_3 \\ t_2 & t_4 \end{bmatrix} \quad \text{and } T^{-1} = \frac{1}{t_4 - t_2 t_3} \begin{bmatrix} t_4 & -t_3 \\ -t_2 & t_1 \end{bmatrix} \tag{4}$$

where T is unknown while R and C are known from the SVD analysis. The coefficients of the T matrix can be determined by TFA (target factor analysis) method as suggested by Lin and Liu (1978).

$$x = [x_1 \quad x_2] = R \begin{bmatrix} t_1 & t_3 \\ t_2 & t_4 \end{bmatrix} = R \begin{bmatrix} t_1 \\ t_2 \end{bmatrix} + R \begin{bmatrix} t_3 \\ t_4 \end{bmatrix} \tag{5}$$

$$x_1 = R \begin{bmatrix} t_1 \\ t_2 \end{bmatrix} \text{ and } x_2 = R \begin{bmatrix} t_3 \\ t_4 \end{bmatrix} \tag{6}$$

x_1 and x_2 are the pure spectra of OP pesticides and its irradiation product respectively. By the known spectrum of OP pesticides, we can calculate t_1 and t_2 with pseudo inverse of the matrix R. But the irradiation product is unknown, so we can not calculate t_3 and t_4 by this method. For this, the sum of concentrations of the two coefficients during the reaction is a constant in the reaction matrix ($C_t = C_1 + C_2$), since t_3 and t_4 can be calculated by:

$$y = [y_1 \quad y_2] = T^{-1}C \tag{7}$$

Using Eqs. (4) and (7), we can calculate the concentration of irradiated OP pesticide. However, there is some ambiguity in the derived results, where, negative values are meaningless. To reduce this rational ambiguity, ITTFA method combined with non-negativity and closure constraints was used. Therefore, to consider zeroing the negative values, a new transformation matrix is obtained as:

$$T = R^{+}x \tag{8}$$

where R^{+} is the pseudo inverse of the matrix R, then Eqs. (7) and (8) can be written as:

$$x = My^{+} \tag{9}$$

To calculate T, x and y matrices, it was repeated iteratively until reaching to convergence. The degree of convergence was determined by two methods; firstly, a comparison of calculated T matrix at each iteration step with that calculated at the previous iteration step and secondly, the difference between the experimental M matrix and the calculated M matrix using x and y matrices.

2.3. Solid phase extraction procedure for OP pesticides in water

The wastewater samples (500 ml) were collected from pesticide industry from Nunhai, Agra (India). All samples were stored in a refrigerator until required. The extraction of OP pesticides from wastewater samples can be isolated, concentrated, and purified. Preconditioning was performed with 2 ml of methanol followed by 2 ml of purified water. Then, 100 ml aliquots of solution were passed through the SPE cartridges (the flow rate was about 2 ml min^{-1}) and finally the retained analytes were eluted with methanol. The organic solution was collected in a 4 ml pre-weighed vial. To this solution, different concentrations; 14, 20, 25, 30 and 40 mg ml^{-1} of OP pesticides (MP and PA) prepared from 100 mg ml^{-1} stock solution (used as an internal standard for HPLC analyses) were added. The samples were then analyzed by HPLC (elution with methanol). The extraction yield and the reproducibility have been determined in the range of 14–40 μg ml^{-1} (this corresponds to a concentration range of MP and PA). The results of percentage recovery from this method and its comparisons with Kubista model is presented in Table 1. Recoveries higher than 72% were obtained for OP pesticides. The mean recovery percentage is obtained using a fixed concentration (40 μg m^{-1}), however, it was significantly different from the value obtained using a set of solutions (range of 14 and 40 μg ml^{-1}). The first set of HPLC values was generally slightly higher than Kubista. The flow rate of the aqueous solution elution should have been optimized for each concentration and this may be the reason for the existence of the observed differences. The set of recovery yields is obtained in the range of 14 and 40 μg ml^{-1}.

2.4. Preparation of ZnO nanoparticles

ZnO nanocatalyst was prepared using the precipitation method. The $ZnSO_4 \cdot 7H_2O$ was used as the starting material and NaOH as precipitant without further purification. The resulting slurry was continuously stirred for 12 h, and then washed with deionized water. The wet powder was dried to form the precursor of ZnO. Finally, the precursor was calcined in air at a certain temperature to produce the nanosized ZnO photocatalyst. The average crystallite or particle size (D in nm) of prepared ZnO nanocrystal was determined by XRD pattern using Debye–Scherrer equation is shown in Fig. 1. The average particle sizes of prepared ZnO are about 35.9 nm (Agarwal et al., 2006).

Table 1 Pesticide conversion at 60 min and rate constant in photocatalytic experiments with different initial concentration.

(Concentration of pesticide in mg ml^{-1})	Methyl parathion (MP)			Parathion (PA)		
	Rate constant	k	r^2	Rate constant	k	r^2
14	0.874	0.028	0.989	0.878	0.026	0.988
20	0.647	0.0218	0.992	0.659	0.0228	0.992
25	0.424	0.0116	0.993	0.413	0.0126	0.993
30	0.369	0.0098	0.992	0.359	0.0089	0.992
40	0.274	0.0072	0.996	0.264	0.0068	0.993

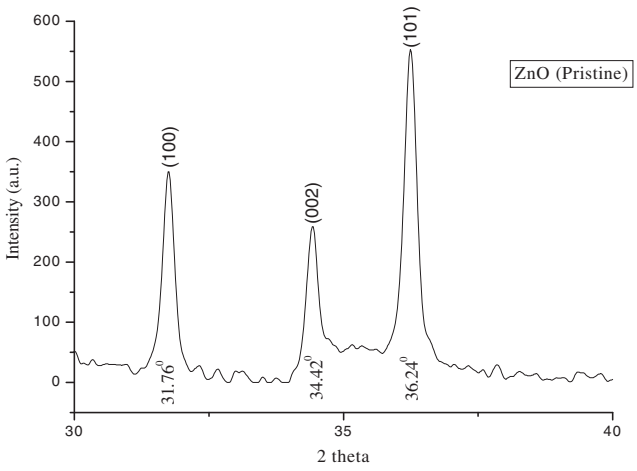

Figure 1 XRD spectra of ZnO nanocatalyst.

$$D = \frac{k\lambda}{\beta Cos\theta} \tag{10}$$

where D is the particle size, λ is the wavelength of X-ray source, β is the FWHM of the peak in XRD-pattern and θ is the scattered angle of the crystallinity. The effect of size on the photodegradation efficiency can be ascribed in two following reasons: (i) the amount of the dispersion of particles per unit volume in the solution will increase, (ii) the resulting enhancement of the photon absorbance at the same time will increase with the surface area of ZnO nanocatalyst, this will extend the adsorption of maximum pesticide molecules on the surface.

2.5. Procedure for degradation assay

For the photodegradation study of pesticides, a solution containing known concentration of the each pesticide and ZnO nanocrystal (size 35.9 nm) was used. It was allowed to equilibrate for 35 min in the darkness, and then 50 ml of the prepared suspension was transferred to a 500 ml Pyrex reactor. Then, the lamp was switched on to initiate the photoreaction. Initially, 15 min was taken to heat the UV lamp before placed the matrix of the sample. To protect external light, irradiation was conducted inside a dark room chamber with UV-source. The light intensity on the surface of pesticide sample was adjusted to 1.0 mW cm^{-2}. During the irradiation the glass reactor mounted on a magnetic stirrer to keep the suspension homogeneous and the suspension was sampled after an appropriate illumination time. The reaction mixtures were kept at the temperature 30 °C. Now, to determine the concentration of pesticide, the samples were filtered through disks to remove ZnO nanocrystal. The concentration of the OP pesticide in each degraded sample in various illumination time was determined using UV–Vis spectrophotometer at λ_{max} = 395 nm for MP and at λ_{max} = 352 nm for PA. The UV–Vis absorbance spectra of OP pesticide (240–430 nm) were recorded in 10 min intervals up to 300 min. At room temperature (27 ± 3 °C), the absorbance data were recorded in 0.5 nm intervals and the data were collected in a data matrix (M). This data matrix was referred to the multivariate curve resolution analysis and reaction rate constants were also calculated.

A Shimadzu HPLC with diode array solvent delivery system controller (LC-10; C_{18} column) was used for all residue analysis of irradiate samples of each insecticide. The injection volume was taken 20 µl, flow rate 1.0 ml min^{-1} and mobile phase 60:40 (acetonitrile/distilled water). To operate HPLC system, Class-VP software is used for data processing. The pH of the samples was adjusted by adding a dilute NaOH and measured by using pH meter.

3. Results and discussion

3.1. Effect of ZnO nanoparticles dosage

The addition of ZnO nanoparticles in photocatalytic system enhances the reaction rate and acts as catalyst. It is attributed to the entrapment of the photogenerated electron, thus it prevents the recombination between electrons and holes. For degradation of OP pesticides in the wastewater, it is necessary to determine the optimum amount of catalyst for the highly efficient degradation. The correlation between the photodegradation efficiency and the concentration of ZnO is shown in Fig. 2. It is observed that when the concentration of the nanophotocatalyst increases from 20 mg l^{-1} to 160 mg l^{-1} at the constant illumination time of 60 min. The rate of degradation was calculated 0.41–0.71 for MP and 0.38–0.69 for PA. Further, as we increase the concentration of nanophotocatalyst beyond 160 mg l^{-1}, no significant changes were observed in degradation. Therefore, the dosage value for which the maximum degradation rate is reached. It indicates an optimal absorption of efficient photons in the UV. Above this value, the scattering phenomena appear and the generation of ZnO($ecb^- + hvb^+$) pairs on the surface of the catalyst loses efficacy that leads to decrease in the degradation rate (Hoffman et al., 1995). An increase in the dosage of nanocatalyst has two different contributions for the photodegradation. Firstly, it makes available a higher number of the nanocatalyst. Secondly, the amount of light dispersed by the nanocatalyst is higher. The optimal conditions for OP pesticides degradation under UV irradiation were obtained as 85 mg l^{-1}.

3.2. Efficiency of nanophotocatalyst

The OP pesticides concentration versus irradiation time profile during the photolysis of MP and PA is described. The photodegradation of OP pesticides was negligible in the absence of ZnO nanocatalyst for the same environmental conditions. The degradation of pesticides was found less than 9 ± 2% in

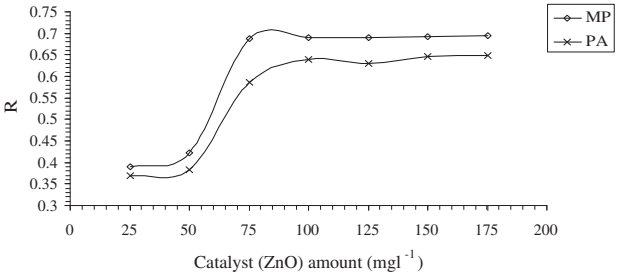

Figure 2 Effect of ZnO nanophotocatalyst on degradation rate (R) of OP pesticides (i.e. MP and PA) in the presence of UV light.

case of direct photolysis that revealed the observed higher decomposition in the UV–ZnO process is due to nanophotocatalytic reaction. It is very clear from Fig. 3a,b that was studied in the presence of UV–ZnO, UV and ZnO pathways. It can also be seen that the 80% removal of the pesticides were observed in 100 min, approximately.

$$ZnO + hv \rightarrow ZnO(ecb^- + hvb^+) \quad (11)$$

$$hv^+ + \text{pesticides} \rightarrow \text{Oxidation of pesticides} \quad (12)$$

$$hvb^+H_2O \rightarrow H^+ + OH^* \quad (13)$$

$$hvb^+OH^- \rightarrow OH^* \quad (14)$$

$$ecb^- + O_2 \rightarrow {}^*O_2^- \quad (15)$$

$${}^*O_2^- + \text{pesticieds} \rightarrow \text{organic peroxides} \quad (16)$$

$${}^*O_2 + HO_2^* + H^+ \rightarrow H_2O_2 + O_2 \quad (17)$$

$$OH^* + \text{organic peroxides} \rightarrow \text{Degradation of pesticides} \quad (18)$$

The results of this experiment show that the effective degradation of OP pesticides has taken place in the presence of UV light and ZnO nanoparticles due to photoexcitation of OP pesticides followed by the formation of an electron–hole ($ZnO(ecb^- + hvb^+)$) pair on the surface of catalyst (Eq. (11)). Since ZnO is a UV sensitive semiconductor and permits the direct oxidation of pesticide to reactive intermediate due to high oxidative potential of hole (Eq. (12)). The formation of free radicals (i.e. hydroxyl radicals) in photocatalytic system is ascribed according to Eq. (13). The free radicals are responsible for degradation of OP pesticides due to their strong non-selective behavior. Electrons in the conduction band (e_{cb}^-) on the nanocatalyst surface can reduce molecular oxygen to superoxide anion (Eq. (15)). This radical, in the presence of organic scavengers, may form organic peroxides (Eq. (16)) or hydrogen peroxide (Eq. (17)). The electrons in the conduction band are also responsible for the production of hydroxyl radicals, which have been indicated as the primary cause of organic matter mineralization (Danehvar et al., 2007). For hypotheses of photodegradation with nanocatalyst, oxygen acts as e_{cb}^- acceptor and reduces the recombination of photogenerated surface electrons with holes, further that improves the efficiency of the photocatalytic process. O_2 adsorbs onto ZnO from the liquid phase where its concentration follows Henery's law. If oxygen is continuously received then its concentration at the surface of ZnO can be assumed constant and therefore, integrated into the apparent rate constant. The fact that this amount of O_2 remains adsorbed after deaeration, suggests a chemisorption process, which is in good agreement with Langmuir isotherm hypotheses.

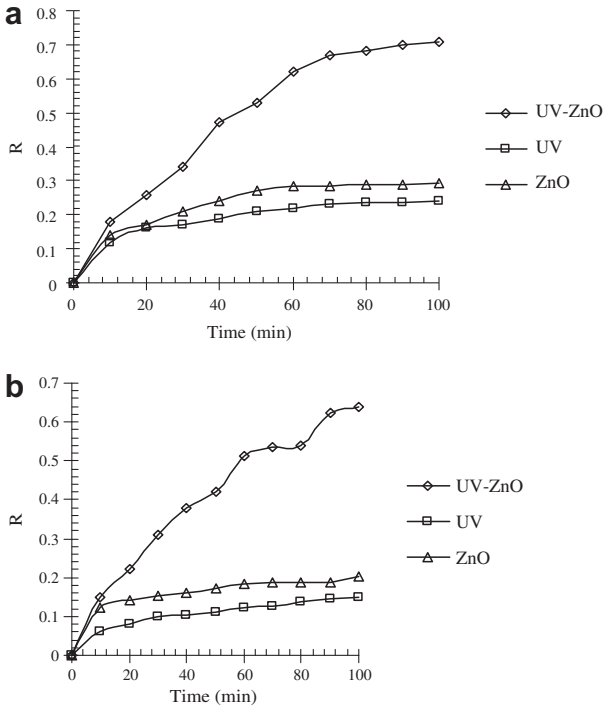

Figure 3 Efficiency of degradation rate (R) on (a) MP and (b) PA in the presence of UV, UV–ZnO and ZnO.

3.3. pH effect

The effect of pH is an interesting variable to evaluate the aqueous phase mediated photocatalytic reactions. To study the suitable correlation at a certain pH, all experimental conditions were kept constant with varying in pH from 3.6 to 10.5 and results are shown in Fig. 4a,b. In acidic medium (pH at 3.6–6.7), these pesticides show the less rate of degradation. Since the pH of ZnO with sample matrix is taken as 9.2, because the surface of the catalyst is positive below at pH 9.2. Therefore, the results in electrostatic attraction between the nanophotocatalyst and pesticides will present the high rate of degradation. But, the electrostatic argument is found very less and shows the concomitant effect. The dissociation constant (pK_a) for MP and PA is 6.83 and 5.21, therefore, MP and

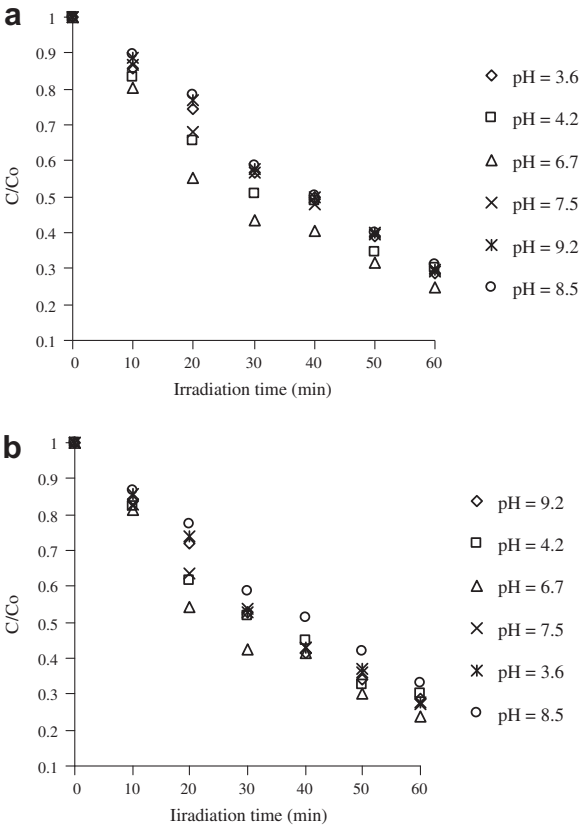

Figure 4 Effect of pH on water samples at different irradiation time intervals, (a) MP, and (b) PA.

PA are negatively charged above pH ~9.0 that might result in electrostatic attraction between the nanocatalyst and pesticides that will increase both adsorption and the degree of photodegradation. It is well known that the ZnO can undergo photocorrosion through self-oxidation, is shown in chemical equations and it has the exhibit tendency to dissolve with decreasing the pH. At high alkaline medium, ZnO can undergo dissolution as reported in the literature.

$$ZnO + 2h^{-}_{vb} \rightarrow Zn^{2+} + 1/2\ O_2 \quad (19)$$

$$ZnO + 2H^{+} \rightarrow Zn^{2+} + H_2O \quad (20)$$

3.4. Effect of water matrix

To investigate the efficiency of UV–ZnO model for removal of pesticides into the water, a 25 ppm of each pesticide was added into the water sample. The primary data of water are carbonate (CO_3^{2-}) hardness 86 mg l^{-1} and sulfate (SO_4^{2-}) concentration 168.8 mg l^{-1}. The effect of presence of common anions such as sulfate, carbonate and bicarbonate on the photocatalytic degradation of pesticides is shown in Fig. 5a,b. It is observed that the rate of degradation decreases in the presence of anions. This inhibition may be hydroxyl radicals (Legrini et al., 1993).

$$SO_4^{2-} + {}^{*}OH^{-} \rightarrow SO_4^{*-} + OH^{-} \quad (21)$$

$$HCO_3^{2-} + {}^{*}OH \rightarrow CO_3^{*-} + H_2O \quad (22)$$

$$CO_3^{2-} + {}^{*}OH \rightarrow CO_3^{*-} + OH^{-} \quad (23)$$

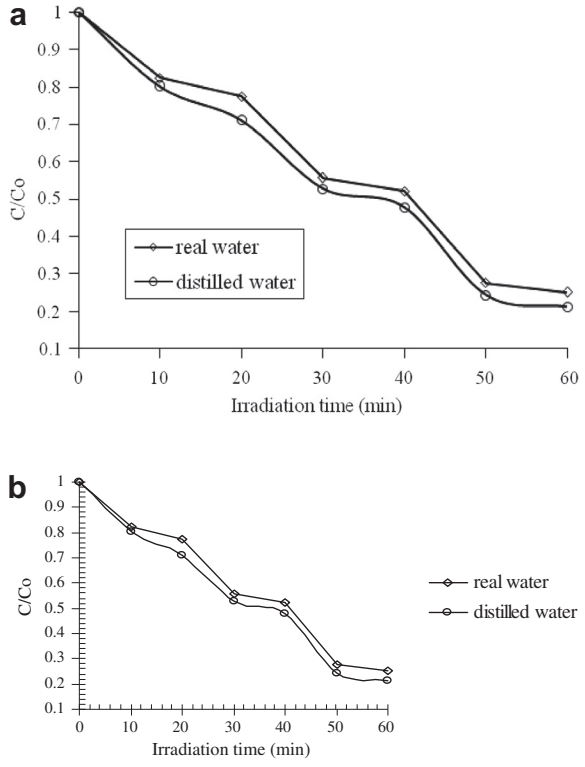

Figure 5 Effect of photocatalytic degradation of pesticides in real water and distill water at pH 9.2, (a) MP and (b) PA.

These anions may stop the active sites on the ZnO surface in intermediate photodegradation process. Although, the generated anions give an oxidant itself, but its oxidation potential is less than for the hydroxyl radicals.

3.5. Kinetics of photocatalytic degradation of pesticides

The photocatalytic degradation of pesticides with nanophotocatalyst follows the pseudo-first order kinetics at low initial pesticide concentration and the rate of expression is:

$$\ln\left[\frac{C}{C_0}\right] = kt \quad (24)$$

where k is the pseudo-first order rate constant, C_o and C are the pesticide concentrations at time $t = 0$ min and $t = t$ min, respectively. Table 1 represents the values of k that was calculated from the plot of $\ln[\frac{C}{C_0}]$ versus irradiation time t for photocatalytic degradation of pesticides. It can be ascribed to the decrease in the number of active sites on the catalyst surface due to the presence of pesticide molecules. The authors have used the modified L–H kinetic model that presents the solid–liquid interfaces (Bolton et al., 2001). The effect of initial concentration of organic substrate on the initial degradation rate (r) is given as:

$$r = \frac{K_p K_c [C]}{1 + K_p [C_0]} = k[C] \quad (25)$$

$$\frac{1}{k} = \frac{1}{K_p K_c} + \frac{[C_0]}{K_c} \quad (26)$$

where K_p and K_c are the L–H adsorption equilibrium constant and the rate constant of surface reaction, respectively. At the lower concentrations up to 40 mg l^{-1}, the L–H equation for the photocatalytic degradation is confirmed by the linear plot between the rate constant ($1/k$) and initial concentration [C_o], is shown in Fig. 6 and Table 1. The values are K_p = 0.127 mg l^{-1} and K_c = 0.212 for MP and K_p = 0.122 mg l^{-1} and K_c = 0.204 for PA, respectively. In view of these results, a fundamental assumption of the L–H mechanism is discussed. The reduction transformation of MP and PA in the absence of oxygen is much less efficient. To explain this, firstly, the reducing power of the electrons in the conduction band is significantly lower than the oxidizing power of the holes in valence band. Secondly, the most reducible substances do not compete kinetically with oxygen in trapping photogenerated conduction band electrons.

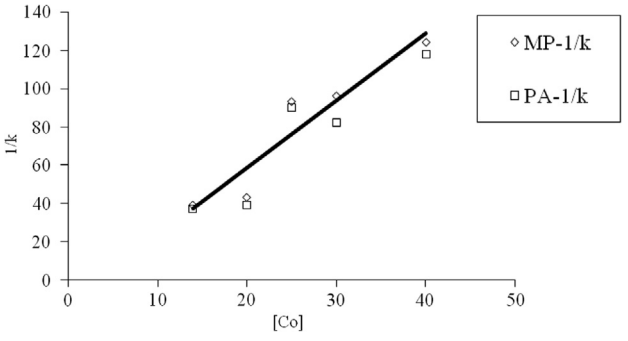

Figure 6 Determination of the adsorption equilibrium constant (K_p) and the kinetic rate constant of the surface (K_c) for the Langmuir–Hinshelwood.

3.6. Electrical energy efficiency

UV–ZnO nanocatalytic process is electric intensive process, and electric energy can represent a major fraction of the operating costs, simple figure-of-merits based on electric energy consumption can be very useful and informative in terms of selecting a waste treatment technology, including economy of scale, regulations, effluent quality aims, operation, and robustness. All these factors are important to design a photoreaction process. The electrical energy per order (E_{EO}) is defined as the number of kilowatt hours of electrical energy required to reduce the concentration of a pollutant in water by 1 order of magnitude in a unit volume of pollutant sample. The E_{EO} (kWh m^{-3} order) could be evaluated from the following equation for a batch type reactor. The E_{EO} (kWh m^{-3}/order) can be calculated from the batch type reactor as:

$$E_{Eo} = \frac{1000Pt}{60V} \log\left[\frac{C}{C_0}\right] \tag{27}$$

where P is the input power (kW) to the AOP system, t is the irradiation time (min), V is the volume of water (in liter) in the reactor, C_o and C are the initial and final concentrations of OP pesticides (Daneshvar et al., 2005; Choy and Chu, 2007).

The E_{EO} values for degradation of pesticide by photolysis of UV–ZnO (35.9 nm) calculated using Eq. (12) are 20,006, 1392.4 kWh m^{-3} for MP and 19,089, 1387.2 kWh m^{-3} for PA, respectively. The E_{EO} values present the electrical efficiency in the photocatalysis process which is better than photolysis model. It also presents that the photocatalysis process in the presence of ZnO nanocatalyst offered the best energy efficiency for the photodegradation of MP and PA.

3.7. Quantum yield

It is defined as the number of molecules being decomposed per photon absorbed. The average photodegradation rate of pesticides concentration C is calculated from the observed first-order degradation rate constant where a specific form of quantum yield based on first-order kinetics is indicated as:

$$\ln\left(\frac{[C]}{[C_0]}\right)_\lambda = -2.303\phi_\lambda I_{0\lambda}\varepsilon_{C\lambda}bt \tag{28}$$

where $[C_0]$ is the initial concentration of pesticide, $[C]$ is the concentration of pesticide at time t, ϕ_λ is the photodegradation quantum yield and $I_{0\lambda}$ (Einstein $I^{-1}s^{-1}$) is the incident light intensity, $\varepsilon_{C\lambda}$ ($cm^{-1}M^{-1}$) is the molar absorptivity at a certain wavelength and b is the optical path length (in cm) (Kuhn et al., 2004; Choy and Chu, 2007; ; Romero et al., 1997; Spadoni et al., 1978). Thus, ϕ_λ can be easily obtained from a plot of $\ln\left(\frac{[C]}{[C_0]}\right)_\lambda$ on time provided, $\varepsilon_{C\lambda}$ and $I_{0\lambda}$ are known.

The quantum yield values for photodegradation of pesticides by direct photolysis and UV–ZnO process under the illumination of UV at 253.7 nm is calculated as 0.00072, 0.012 for MP and 0.00068, 0.01 for PA. It is clear from observed values that the ZnO-quantum yield is higher than direct photolysis. It means that the photodecay of MP and PA is highly dominated by ZnO nanocrystal as compared to direct photolysis.

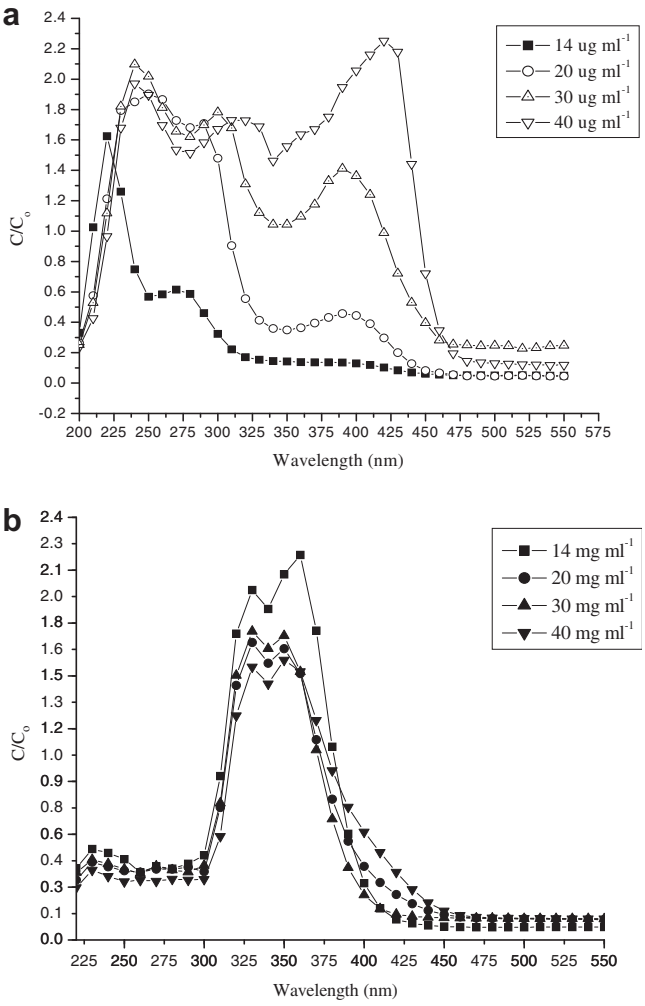

Figure 7 Quantitative analysis of (a) MP and (b) PA by UV–Vis spectrophotometer using Kubista model at the wavelength interval of 10 nm.

3.8. HPLC analysis

The peak area of HPLC chromatograph was calculated before and after the irradiation process. These data provides a series of confirmative results as a standard chromatographic technique for quantitative analysis of pesticides. The HPLC analysis begins with injection of the sample into the instrument with a syringe. The extracted sample of highly toxic pesticide from waste water is first vaporized at high temperature (200–350 °C) in the injection port and then forced onto the separating column by a carrier gas. The carrier gas serves as the mobile phase for this chromatographic separation. The stationary phase is a very thin layer of a polymeric material that was coated inside the column. A range of polymer coatings with varying polarities are available and a correct coating must be chosen for successful analysis.

3.9. UV–Vis spectrometry coupled with Kubista model

The irradiation of OP pesticide is studied in different ways with chromatographic methods but they have no sufficient data to understand kinetics of reaction mechanism. In present

Table 2 A comparative data for analysis of OP pesticides between UV–Vis coupled with Kubista model and HPLC techniques.

OP pesticides	Concentration of OP pesticides in μg ml^{-1}	Kubista model			HPLC		
		Recovery (1.5 ± SD)[a]	Recovery (2.5 ± SD)[b]	% ±0.5 RSD	Recovery (1.5 ± SD)[a]	Recovery (2.5 ± SD)[b]	% ± 0.5 RSD
MP	14	93.8 ± 2	93.8 ± 3	2	98.2 ± 3	98.2 ± 4	5
	20	92.8 ± 5	92.8 ± 4	4	93.4 ± 5	97.4 ± 8	3
	25	93.0 ± 1	93.0 ± 2	5	91.5 ± 9	98.5 ± 6	6
	30	92.4 ± 6	92.4 ± 5	6	94.4 ± 12	97.4 ± 4	4
	40	91.3 ± 3	91.3 ± 4	3	93.2 ± 8	98.2 ± 5	3
PA	14	94.4 ± 5	94.4 ± 2	3	98.2 ± 4	98.2 ± 3	6
	20	93.2 ± 4	93.2 ± 5	2	93.4 ± 7	97.4 ± 4	3
	25	93.6 ± 2	93.6 ± 6	4	92.5 ± 9	98.5 ± 6	3
	30	92.9 ± 3	92.9 ± 5	5	93.4 ± 8	98.4 ± 5	2
	40	92.8 ± 5	92.8 ± 7	2	93.2 ± 7	99.2 ± 9	4

[c] Relative standard deviation estimated using a signal-to-noise ratio of 5.
[a] Mean value and SD obtained with eight extractions of aqueous solution (40 μg ml^{-1}).
[b] Mean value and SD obtained with a set of solutions containing eight concentrations range 14–40 μg ml^{-1}).

work, we are first time reporting a multivariate curve resolution method for study of OP pesticide using nanophotocatalyst. We found that the chromatographic methods were not sufficient for studying the kinetics of such reaction. In this study, we applied Kubista model for kinetics of photoinduced reaction. The reaction rate constant can be evaluated directly from the resulting concentration–time profiles by fitting the first segment to a linear model and second segment to an exponential model. The pure absorbance spectra of the components and their corresponding concentration profiles were determined by the Kubista method (target transformation factor analysis). The resolved spectra for each pesticide similar to that obtained experimentally, are shown in Fig. 7a,b. Therefore, the data are written in Matlab and calculated the effective parameters. The equation obtained for the linear (C_f) and exponential segments (C_s) which are calculated using Eqs. (6)–(9) for MP and PA is:

$$\text{for MP; } C_f = 1.116(\pm 0.001)\times 10^{-4} - 2.39(\pm 0.13)\times 10^{-9}t;\ r^2 = 0.987;$$
$$C_s = 1.102(\pm 0.002)\times 10^{-4} \quad \exp \quad (-5.22(\pm 0.08)\times 10^{-5}t);\ r^2 = 0.984$$
$$\text{for PA; } C_f = 1.116(\pm 0.001)\times 10^{-4} - 2.39(\pm 0.13)\times 10^{-9}t;\ r^2 = 0.987$$
$$C_s = 1.102(\pm 0.002)\times 10^{-4} \quad \exp \quad (-5.22(\pm 0.08)\times 10^{-5}t);\ r^2 = 0.984$$

The linear (C_f) and exponential segments (C_s) showed that there are two chemical compounds that take part in the reaction system in which one of them is parent pesticides and another one is the photodecomposition product of the parent pesticides. The concentration of the pesticides in each degraded sample in various illumination time was determined by UV–Vis spectrophotometer at λ_{max} = 395 nm for MP and at λ_{max} = 352 nm for PA. The applied process is suitable for the removal of OP pesticides using UV–ZnO nanocatalyst. The removal technique for OP pesticides was achieved at certain experimental conditions. In most cases, *p*-nitrophenol and esters were obtained during degradation of OP pesticides and can be verified with UV–Vis peak at 279 nm. Therefore, the results calculated by UV–Vis spectroscopy coupled with Kubista model that was further validated by HPLC data with ±2.5% error, are presented in Table 2. These findings demonstrate that the oxidative reactivity with different members in a specific class of pesticides can vary significantly due to chemical structure variations.

4. Conclusion

The optimal conditions for MP and PA degradation under UV irradiation were obtained using ZnO nanocatalyst at 85 mg l^{-1}, required oxygen demand of 40% with rate constants L–H adsorption equilibrium constant (K_p = 0.127 for MP and 0.122 for PA) and rate constant of surface reaction (K_c = 0.212 for MP and 0.204 for PA). Under such conditions, a 93 ± 2.5% degradation of MP and PA was achieved. It also proves more efficient photonanocatalyst for the oxidation and decomposition of the pesticides proceeded at higher reaction rates. The photodegradation of MP and PA has several merits such as: (i) in the presence of ZnO nanoparticles or UV light the degradation of pesticides is negligible, (ii) the rate of degradation of pesticides is affected by the illumination time, pH and photocatalyst loading, (iii) The electrical energy consumption per order of magnitude for photocatalytic degradation of pesticides is found to be less than direct photolysis, (iv) The ZnO nanoparticles offer the highest quantum yield than direct photolysis and (v) The kinetics of photocatalytic has also showed a good response for removal of OP pesticides (MP and PA) by L–H model. The multivariate curve resolution method is based on the combination of Kubista approach and iterative target transformation method was applied to study the kinetics of OP pesticides. In this method, we found that the kinetic profile of the degradation of OP pesticides possesses two regions. The first region is linear with time which confirms a zero order kinetic and the second region showed a first-order kinetic pathway that followed the two products in which one is remaining part (~11.2%) of parent OP pesticides concentration and another one is photodecomposition product of parent OP pesticides in the reaction system. A detailed discussion of nanocatalyst operation for photodegradation process was also concluded.

Acknowledgements

Authors express their gratitude to the Department of Science & Technology, New Delhi, Government of India for financial support. Authors are also thankful to The Director, Hindustan College of Science and Technology, Farah, Mathura 281122 (U.P.), India. We are also thankful to Dr. R.J. Chaudhary, Scientist, UGC-DAE, Consortium for Scientific Research, Indore, India to provide the XRD measurement and Dr. M.S. Thakur, Scientist, Fermentation Technology and Bioengineering Department, Central Food Technological, Research Institute, Mysore 570020, Karnataka, India, for HPLC measurement.

References

Agarwal, D.C., Chauhan, R.S., Kumar, A., Kabiraj, D., Singh, F., Khan, S.A., Avasthi, D.K., Pivin, J.C., Kumar, M., Ghatak, J., Satyam, P.V., 2006. Synthesis and characterization of ZnO thin film grown by electron beam evaporation. J. Appl. Phys. 99, 123105–123110.

Bolton, J.R., Bircger, K.G., Tumas, W., Tolman, C.A., 2001. Fig.-of merit for the technical development and application of advanced oxidation technologies for both electric and solar-derived systems. Pure Appl. Chem. 73, 627–637.

Canle, M.L., Rodriguez, S., Rodriguez, V.L.F., Santaballa, J.A., Steenken, S., 2001. First stages of photodegradation of the urea herbicides Fenuron, Monuron and Diuron. J. Mol. Struct. 565, 133–139.

Cassano, A.E., Martin, C.A., Brandi, R.J., Alfano, O.M., 1995. Photoreactor analysis and design: fundamentals and applications. Ind. Eng. Chem. Res. 34, 2155–2201.

Choy, W.K., Chu, W., 2007. The use of oxyhalogen in photocatalytic reaction to remove o-chloroaniline in TiO_2 dispersion. Chemosphere 66, 2106–2113.

Chandrasekhar, S., 1960. Radiative Transfer. Dover New York.

Doong, R., Chang, W.J., 1997. Photoassisted titanium dioxide mediated degradation of organophosphorus pesticides by hydrogen peroxide. Photochem. Photobiol. A: Chem. 107, 239–244.

Dannenberg, A., Pehkonen, S.O., 1998. Investigation of the heterogeneously catalyzed hydrolysis of organophosphorus pesticides. J. Agric. Food Chem. 46 (1), 325–334.

Diaz-Cruz, M.S., Mendieta, J., Tauler, R., Esteban, M., 1999. Multivariate curve resolution of cyclic voltammetric data: application to the study of cadmium binding properties of glutathione. Anal. Chem. 71, 4629–4636.

Danehvar, N., Aber, S., Seyed Dorraji, M.S., Khataee, A.R., Rasoulifard, M.H., 2007. Preparation and investigation of photocatalytic properties of ZnO nanocrystals: effect of operational parameters and kinetic study. Sep. Purif. Technol. 58, 91–98.

Daneshvar, N., Aleboyeh, A., Khataee, A.R., 2005. The evaluation of electrical energy per order (E_{Eo}) for photooxidative decolorization of four textile dye solutions by the kinetic model. Chemosphere 59, 761–767.

Eleni, E., Ioannis, K., Konstantinos, F., Ioannis, P., Triantafyllos, A., 2007. Photocatalytic oxidation of methyl parathion over TiO_2 and ZnO suspensions. Catal. Today 124, 156–162.

Feed, V.H., Chiou, C.T., Schmedding, D.W., 1979. Degradation of selected organophosphate pesticides in water and soil. J. Agric. Food Chem. 27 (4), 706–708.

Fouassier, J.P., 1989. Excited-state properties of photoinitiators: lasers and their applications. In: Norman, A.S. (Ed.), Photopolymerization and Photoimaging Science and Technology. Elsevier, London, New York.

Frans, S.D., Harris, J.M., 1985. Least squares singular value decomposition for the resolution of pK's and spectra from organic acid/base mixtures. Anal. Chem. 57 (8), 1718–1721.

Gooijer, C., Mank, A.J.G., 1989. Quantitation of sodium hydrogensulfite in parenteral samples by a flow-injection method. Anal. Chim. Acta 220, 281–285.

Gemperline, P.J., 1986. Target transformation factor-analysis with linear inequality constraints applied to spectroscopic chromatographic data. Anal. Chem. 58, 2656–2663.

Han, B., Ko, J., Kim, J., Kim, Y., Chung, W., Makarov, I.E., Ponomarev, A.V., Pikaev, A.K., 2002. Combined electron beam and biological treatment of dying complex waste water: pilot plant experiments. Radiat. Phys. Chem. 64, 53–59.

Hoffman, M.R., Martin, S.T., Choi, W., Bahnemann, D.W., 1995. Environmental applications of semiconductor photocatalysis. Chem. Rev. 95 (1), 69–96.

Kankare, J.J., 1970. Computation of equilibrium constants for multicomponent systems from spectroscopic data. Anal. Chem. 42, 1322–1326.

Kuhn, H.J., Braslavsky, S.E., Schmidt, R., 2004. Chemical actinometry, IUPAC technical report. Pure Appl. Chem. 76, 2105–2146.

Lopez, J.L., Einsclag, Garcia, F.S., Gonzalez, M.C., Capparelli, A.L., Oliveros, E., Hashem, T.M., Braun, A.M., 2000. Hydroxyl radical initiated photodegradation of 4-chloro-3, 5-dinitrobenzoic acid in aqueous solution. J. Photochem. Photobiol. A: Chem. 137 (2–3), 177–184.

Lopez, A., Bozzi, A., Mascolo, G., Kiwi, J., 2003. Kinetic Investigation on UV and UV/H_2O_2 degradation of pharmaceutical intermediates in aqueous solution. J. Photochem. Photobiol. A: Chem. 36, 121–126.

Lavine, B.K., 2000. Chemometrics. Anal. Chem. 72, 91R–97R.

Lawton, W.H., Sylvestre, E.A., 1971. Elimination of linear parameters in nonlinear regression. Technometrics 13, 461–467.

Lin, C.H., Liu, S.C., 1978. A new numerical method for automated spectral isolation of component substances in a set of mixtures. J. Chin. Chem. Soc. 25, 167–177.

Legrini, O., Oliveros, E., Braun, A.M., 1993. Photochemical processes for water treatment. Chem. Rev. 93, 671–698.

Malinowski, E.R., 1991. Factor analysis in Chemistry, second ed. Wiley, New York.

Nicole, I., Latt, J.D., Dore, M., Duguet, J.P., Bonnel, C., 1990. Use of UV Radiation in water treatment: measurement of photonic flux by hydrogen peroxide actinometry. Water Res. 24 (2), 157–168.

Ollis, D.F., Al-Ekabi, H., 1993. Photocatalytic Purification and Treatment of Water and Air. Elsevier, Amsterdam.

Pehkonen, S.O., Zhang, Q., 2002. The degradation of organophosphorous pesticides in natural waters: a critical review. Environ. Sci. Technol. 32 (1), 17–72.

Pikaev, A.K., Makarov, I.E., Ponomarev, A.V., Kim, Y., Han, B., Yang, Y.W., Kang, H.J., 1997. A combined electron beam and coagulation method of purification of eater from dyes. Mandeleev Commun. 5, 176–178.

Primo, O., Rivero, M.J., Ortiz, I., Irabien, A., 2007. Mathematical modelling of phenol photooxidation: kinetics of the process toxicity. Chem. Eng. J. 134, 23–28.

Pareek, V.K., Brungs, M.P., Adesina, A.A., 2001. Continuous process for photodegradation of industrial bayer liquor. Ind. Eng. Chem. Res. 40, 5120–5125.

Racke, K.D., Chembers, J.E., Levi, P.E., 1992. Organophosphorus Chemistry, Fate and Effects. Academic Press, San Diego, pp. 47–73.

Romero, R.L., Alfano, O.M., Cassano, A.E., 1997. Cylindrical photocatalytic reactors: radiation absorption and scattering effects produced by suspended fine particles in an annular space. Ind. Eng. Chem. Res. 36, 3094–3109.

Salari, D., Daneshvar, N., Aghazadeh, F., Khataee, A.R., 2005. Application of artificial neural networks for modeling of the treatment of wastewater contaminated with methyl tert-butyl ether (MTBE) by UV/H_2O_2 process. J. Hazard Mater. 125, 205–210.

Sharma, A.K., Gaur, K., Tiwari, R.K., Gaur, M.S., 2011. Computational interaction analysis of organophosphorus pesticides with different metabolic proteins in humans. J. Biomed. Res. 25, 335–347.

Shrager, R.I., 1986. Chemical transitions measured by spectra and resolved using singular value decomposition. Chemom. Intell. Lab Syst. 1, 59–70.

Spadoni, G., Bandini, E., Santarelli, F., 1978. Scattering effects in photosensitized reactions. Chem. Eng. Sci. 33, 517–524.

Stephen, C., Stefan, M.I., Bolton, J.R., Safazadeh, A., 2000. Degradation pathways during the treatment of methyl tert-butyl ether by the UV/H_2O_2 process. Environ. Sci. Technol. 34, 650–658.

Sulaiman Gafar Muhamad, 2010. Kinetic studies of catalytic photodegradation of chlorpyrifos insecticide in various natural waters. Arabian J. Chem. 3 (2), 127–133.

Trebse, P., Franko, M., 2002. Laser-induced degradation of organophosphorus compounds. Int. J. Photoenergy 4 (1), 41–44.

Zhang, Q., Pehkonen, S.O., 1999. Oxidation of diazinon by aqueous chlorine: kinetics, mechanisms, and product studies. J. Agric. Food Chem. 47, 1760–1766.